This is the Pre-Published Version.

This document is the Accepted Manuscript version of a Published Work that appeared in final form in Crystal growth and design, copyright © 2018 American Chemical Society after peer review and technical editing by the publisher. To access the final edited and published work see https://doi.org/10.1021/acs.cgd.8b00806.

In Situ Observation of Ice Formation from Water Vapor by Environmental SEM

Zhouyang Zhang,† Linfeng Fei,*,‡ Zhenggang Rao,† Dingjun Liu,§ C. W. Leung,‡ and Yu Wang*,†

† Department of Materials Science and Engineering, Nanchang University, Jiangxi 330031, China

‡ Department of Applied Physics, The Hong Kong Polytechnic University, Hong Kong SAR, China

§ Institute of Advanced Sciences, Nanchang University, Jiangxi 330031, China

Corresponding Authors

*E-mail: feilinfeng@gmail.com (L.F.).

*E-mail: wangyu@ncu.edu.cn (Y.W.).

Abstract

A microscopic understanding of the mechanism of direct ice formation from water vapor has a significant benefit for controlling the processes involving ice condensation and evaporation. However, previous studies on this topic have been limited to theoretical simulations or optical observations. Here, by in situ observation via environmental scanning electron microscopy (ESEM), we revealed that hexagonal ice crystals are developed by a step-by-step pathway in a supersaturated water vapor environment. Furthermore, we also discerned that such steps came from two different origins, which are screw dislocations and initial steps. In addition, the relationship between the edge-length (of hexagonal ice crystals) and the growth time was quantitatively studied at controlled temperatures and pressures by experimental data fitting. This study shows that qualitative and quantitative observations of ice formation can be made with simple setups, and it should inspire future investigations toward important physicochemical processes using ESEM, especially those that simultaneously involve two or more phases.

Introduction

Ice formation is a common phenomenon and has widespread influence over both industrial processes and our daily life. (1−4) In fact, the process of formation for an ice crystal (a snowflake) from the gaseous phase is complicated and is primarily determined by two parameters: temperature (*T*) and water vapor supersaturation (σ). (5−9) The beginning of scientific studies on icing dates back to the early 1930s, during which cameras or optical microscopes were employed to observe such processes. For example, on the basis of decades of research by taking thousands of photos on snow crystals, Humphreys et al. claimed that there were no two identical snowflakes in the world. (10) Then, Nakaya, who first created artificial snow in the laboratory, observed different growth patterns of snow crystals at different temperatures and supersaturation levels, and the results have been plotted in the famous "snow crystal morphology diagram". (11,12) On the basis of Nakaya's general classification, Magono developed a more detailed and the most widely accepted account on snow shapes, including 76 patterns such as needle, plate, sheath, and so on. (13) A fundamental ice crystal form is a hexagonal prism, consisting of two basal facets {0001} and six prism facets $\{10\bar{1}0\}$. (14) Thereafter, qualitative and quantitative studies were carried out to understand the growth process of ice, which is simply divided into three stages (crystal growth stage, ice-layer growth stage, and ice-layer full growth stage). (15) Other parameters were also studied, including the influence of mass transfer, moisture content, and cold surface temperature on icing rate, (16) as well as the structures of the ice-layer under different icing conditions. (17) There were also a few reports focusing on the icing mechanisms. In 1989, Yokoyama and Kuroda proposed a simulation model of pattern formation with three types of snow crystal patterns (circular pattern, hexagonal pattern, and dendritic pattern), based on both the surface kinetic

process and the diffusion process. (18) For the disk crystals, Shimada et al. found that their three-dimensional growth pattern could be categorized into two types depending on the presence of screw dislocations by *in situ* observations using an interferometric optical system. (19) On the basis of the terrace–ledge–kink model, Wood presented a new physical model in which ledges (steps) were created either by outcropping of screw dislocations or by two-dimensional nucleation. (20) Libbrecht described the influence of edge-sharpening instability in diffusion-limited vapor growth on the formation of thin plates at −15 °C. (21)

The research interest in icing has been revived in this century, as a consequence of the rapid advancement on computational physics as well as observational techniques. (22−25) Recently, scientists were also able to monitor the icing process by a range of *in situ* techniques, allowing direct studies concerning the formation of ice on different surfaces with different wettability. Wu et al. observed the complete process of freezing a droplet and the different macroscopic structures of ice, using a microscopic image system consisting of a zoom stereo microscope, a CCD camera, an image processor, and a self-built program. (26,27) Liu et al. imaged the growth process of six-leaf clover-like ice on hydrophobic surfaces to investigate the growth of ice crystals on different solid surfaces and the relationship between the growth process and the contact angle, using an optical microscope coupled with a high-speed camera. (28)

On the other hand, state-of-the-art computation techniques showed considerable deviations with the experimental observations due to the limitation of the simulated system. For example, Reiter proposed a 2-dimensional model to investigate the impact of various growth conditions, which failed to express the actual three-dimensional forms of snow crystals. (29) Moreover, we note that many existing reports have attributed the ice formation to supercooled droplets; nevertheless, the growth kinetics and mechanism of ice crystal or ice-layer is not fully

understood. (26,27,30−32) We suggest that a microscopic study on morphological changes during the crystal growth stage and ice-layer development arising from the deposition of water vapor are crucial for constructing the complete scenario of the icing process, as well as the final control over icing in certain circumstances (artificial ice making, aircraft icing management, etc.).

Following our previous *in situ* studies on crystal growth, (33−36) we extend our research to the observation of crystallization of water (i.e., ice forming) via environmental scanning electron microscope (ESEM) in this work. (37−42) With the development of ESEM, unparalleled opportunities have been provided to carry out direct and high-resolution observations concerning microstructural changes or microscale reactions in controlled environments, for example, the evolution of water droplets during wetting process and nanoscale ice crystal formation. (43−46) Therefore, in this work, we accurately control the temperature and relative humidity over a broad range inside the ESEM chamber and directly observe the consequent icing process. As will be demonstrated later in the paper, this work has revealed the microstructure and growth pattern of ice crystals and the formation process of the ice-layer, which has further led to a theoretical discussion on the growth dynamics. Our studies provide valuable insights into the mechanisms of ice formation and morphological change during the growth and will be beneficial for understanding ice crystal growth from the gaseous phase in a fundamental manner.

Experimental Methods

ESEM (Quanta 200F, FEI, U.S.) was used to observe the icing process in a series of water vapor pressures and chamber temperatures (as described in the following text). The working distance was set as 15 mm, and the electron spot was 3.0. The voltage was 20 kV, and the working mode was ESEM mode. The icing temperature was controlled by a cooling stage assembly within the

ESEM chamber, while the supersaturation of water vapor was controlled by the chamber pressure (in this case the low-pressure water vapor can be treated as ideal gas).

Results and Discussion

Microscopic Growth of Ice Crystal

We performed a series of *in situ* experiments in ESEM to observe the growth of ice crystal under controlled temperatures and water vapor pressures (Figure S1–S6) and found that the growth of ice crystal was intimately related to temperature (T) and supersaturation (σ). The increase of σ can accelerate the growth under a certain T, and σ must increase when T decreases. (5,6) Results of a representative experiment ($T = -15$ °C, $P = 179$ Pa, $\sigma = 0.86\%$) are shown in Figure 1 to demonstrate the growth process of an ice crystal. Initially, when the water molecules in the gaseous phase with a high supersaturation deposit on a supercooled surface, they preferentially nucleate at some points where surface defects (such as dust particles or rust spots) act as heterogeneous nucleation centers to form embryos, as shown in Figure 1a. Subsequently (Figure 1b,c), as the embryo grows, it becomes anisotropic and forms a hexagonal prism that follows the crystal structure of ice.

For an ideal hexagonal prism, there are two kinds of facets, i.e. six prism facets ($\{10\bar{1}0\}$ facets) and two basal facets ($\{0001\}$ facets) as shown in Figure 1d. In principle, after the formation of an ice hexagonal prism as in Figures 1c and 2a, the further growth is dominated by the lattice anisotropy of the ice crystal. The six prism facets, represented as the closest packing direction in the atomic structure of ice, are more unstable and hence have higher growth rates than the two basal facets. Actually, we did not observe any significant change in the basal facet as shown in Figure 2b–d, except for the formation of a certain degree of surface roughness. In contrast, the

six identical prism facets change significantly during the observation. The prism facets grow outward by means of forming layered steps, called initial steps, perpendicular to the *c* axis, while each initial step is composed of a number of connected quasihexagonal micropieces (Figure 2e–g). The continuous deposition of water molecules from gaseous phase onto the microstructure of the ice crystal leads to fast in-plane growth of the prism, which should be a result of the energy competition between different crystal facets.

Step-by-Step Growth of Ice-Layer

During further observation, we saw that several crystals (Figure 2a) horizontally met each other, merged into a big one, and then formed a bicontinuous ice-layer on the substrate. Observation was carried out to understand the growth fashion of the ice-layer, as recorded in Movie S1, and Figure 3 summarizes the structural evolution of the ice-layer with respect to time. Throughout the entire ice-layer formation process, the basic growth units are steps, as shown in Figure 3a. As mentioned above, this "ice-layer" process happens after the previous "crystal" process. For a crystal, during the ice-layer formation, its initial steps and micropieces (Figure 2) develop into some steps and screw dislocations. Additionally, screw dislocations are always formed upon extrusion of neighboring ice crystals. Therefore, it can be concluded that the step-by-step growth of the ice-layer mainly proceeds via two structures, screw dislocations (denoted as 1 in Figure 3a) and steps (denoted as 2 in Figure 3a). Figure 3b–d shows how screw dislocations grow and move. Water molecules from the vapor are the resources for the growth, and the dislocation head leads the growth due to energy reasons. Such growth may be stopped by neighboring steps or be influenced by internal strains. As the solidification process goes on, dislocations may disappear, and finally, the ice steps become the dominant form of microstructure. Figure 3e–g shows how the ice-layer grows. Again, water molecules from the

vapor are the resources for the growth, and step edges lead the growth due to the edge-sharpening instability; considering that the supersaturation is the highest near the step edge (namely, Berg effect), the water molecules therefore prefer to be deposited on the step edges. (21) Through the direct observation, one can see that the growth rate along the lateral directions of a step is much larger than that of the step thickness, and several steps could merge into one thicker stage (as shown in Figure 3h, with h2 and h3 becoming h2(3)′. The whole process is schematically illustrated in Figure 3h.

The microscopic understanding of the icing mechanism has been continuously refined over the past few decades. In the 1960s, Ketcham reported that, in pure water, the cooling interface can propagate in the form of steps which originate from grain boundaries and spiral sources. (47) Recently, Lamb et al. proposed a growth model, suggesting that both the basal and the prism facets are due to the propagation of spiral steps developed from screw dislocations. (48) Using MD simulation, Nada et al. discovered that the structure of the ice/water $\{0001\}$ interface was smooth, whereas the ice/water $\{10\bar{1}0\}$ interface was rough. (49) In 2001, a new model for the growth mechanism of steps with both two-dimensional nucleation and spiral dislocation was proposed, in order to describe the process observed by Wood et al. (20) Upon further studies, Libbrecht claimed that edge-sharpening instability can promote the formation of ice, and the water molecules prefer to be absorbed on the corner of step edges of ice crystals. (21) In contrast, in this work, we discerned new details in the microscopic icing mechanism with ESEM, in which the prism facets in hexagonal ice crystal were developed through stacking of multiple steps, while each step was composed of many quasihexagonal pieces. We also observed that growth of steps first started at every corner of the steps and then spread over the surfaces. For the ice-layer formation, the steps from either initial ones or screw

dislocations led to the step-by-step growth of ice. Moreover, we also observed that growth of steps first started at every edge of the steps, which was followed by a spreading over the flat surfaces (Movie S1).

Kinetic Analysis of Ice Growth

In this work, ice formation is a phase transition of water from vapor to solid, on the condition that water molecules in the gaseous phase come across a cold surface. According to the fundamental equation of thermodynamics: $\mathrm{d}G = -S\,\mathrm{d}T + V\,\mathrm{d}p$ (1)When the temperature of the system is fixed (dT = 0), the variation of the Gibbs function in the process of desublimation can be expressed as

$$\Delta G = \int_{p}^{p_e} V\,\mathrm{d}p \tag{2}$$

where p is the actual water vapor pressure in the environment and p_e is saturated water vapor pressure on the ice surface. Considering water vapor as a perfect gas, it follows that the ideal gas equation

$$pV = nRT \tag{3}$$

and according to eq 2

$$\Delta G = \int_{p}^{p_e} \frac{nRT}{p}\mathrm{d}p \tag{4}$$

after integral operation

$$\Delta G = nRT \ln \frac{p_e}{p} \tag{5}$$

and according to Tetens' empirical formula, (5) the saturated vapor pressure on ice surface can be calculated by

$$p_e = 611 \times e^{\frac{9.5T'}{265.5 + T'}} \tag{6}$$

where T' is Celsius temperature. According to eq 5, $\Delta G < 0$ when $p > p_e$. In this case, the rate of water molecules moving from air to ice is higher than that of water moving away from ice to air. To observe the ice formation, we controlled the water vapor pressure of ESEM under this condition. In order to explore the regular pattern of speed variation, some statistical data were measured from the captured ESEM micrographs in order to describe the kinetics during the ice growth. Also, this process can be described with diffusion, such that the velocity of the crystal growth (v) can be expressed with the rate of change in crystal's mass (m) according to Fick's first law:

$$v = \frac{dm}{dt} = -DA\frac{d\rho}{dx} \tag{7}$$

where D is the diffusion coefficient, ρ is the mass concentration, and $\frac{d\rho}{dx}$ is the concentration gradient in the direction of diffusion x. A is the area, and the minus sign expresses that the direction of diffusion is opposite to the direction of concentration gradient. From eqs 3 and 7

$$v = -\frac{DMA}{RT}\frac{dP}{dx} \tag{8}$$

Here, M is molar mass. In this process, v can be written in the following form:

$$v = -\frac{DMA}{RT}(p - p_e) = -\frac{DMA}{RT}p_e\sigma \tag{9}$$

In our work, the velocities under different temperatures (T) and varying degrees of supersaturation (σ) are discussed in Figure 4a. According to eq 9, we fit the data with a linear function, and consequently, the slopes of the linear fits for data at −12, −13, −14, −15, −16, −20, and −22 °C are 0.203, 0.367, 0.488, 0.484, 0.423, 0.398, and 0.327 μm/s, respectively. Interestingly, it is obvious that the ice grows fastest when the temperature is at −14 °C, at which point this process can take place most easily. According to the previous study, the only possibility for this phenomenon is the existence of a quasi-liquid-layer on the ice surface caused by premelting. (50,51) This regular pattern gives indirect proof that there is an occurrence of premelting on the ice/vapor interfaces of the ice crystal, namely, the existence of a quasi-liquid-layer. (52,53) In the surface quasi-liquid-layer, the connection between water molecules is much looser than that of internal molecules (solid ice). At higher temperatures (>−14 °C in our case), the quasi-liquid-layer tends to be a continuous liquid layer on the ice surface, and the interface (ice/vapor) becomes smoother, so the water molecules in vapor are very difficult to be adsorbed into the ice body, resulting in the decrease of ice growth rate. On the contrary, at lower temperatures (<−14 °C), surface-melting is largely prohibited, and therefore, the ice/vapor interface is also very smooth (caused by the close molecule arrangement in solid ice), leading to slower adsorption of water molecules and the slower growth rate. Only if the temperature is at a critical point (= −14 °C) will a suitable distribution of quasi-liquid-layer on the ice surface make the water molecules in vapor much easier to be adsorbed and, hence, can boost the speed of ice growth.

For more intuitive comparison of ice growth at different temperatures, Figure 4b, depending on the results of linear fitting, demonstrates the dependence of σ (at a given v = 2 μm/s) and v (at a

given σ = 12) on *T*. In addition, for our chosen single crystal with the morphology of a plate-like hexagonal prism, the area of a basal facet can be calculated by

$$A = \frac{3\sqrt{3}a^2}{2},$$

where *a* is the edge-length of the hexagon, and its thickness does not change with time, considering eqs 7 and 9, in the crystal growth

$$\frac{dm}{dt} = -\frac{DM3\sqrt{3}p_e\sigma}{2RT}a^2 \quad (10)$$

Hence, the time dependence of the edge-length of an ice crystal at a constant temperature is described as $a \propto \sqrt{t}$. In our experiment, the change of edge-length of the basal facet with time at different temperatures (−14 and −15 °C) at a given σ is shown in Figure 4c, and Figure 4d is the data at −18 °C (σ = 8.65%). The results all show good linear relationships, which is consistent with the theoretical calculations; moreover, the crystal growth rate at −14 °C is the fastest at a given σ, also in line with Figure 4a,b.

Conclusion

We reported *in situ* ESEM analysis of direct ice formation from a supersaturated water vapor environment. The results show that the steps, which come from two distinct paths (screw dislocations and initial steps), play very important roles during the whole ice formation process. Ice crystals, in the form of hexagonal plates, can be anisotropically developed through the addition of these microscopic steps. Moreover, by careful theoretical derivation and experimental data fitting, the relationship between edge-length *a* of hexagonal ice plates against time *t* at a constant temperature is determined as $a \propto \sqrt{t}$, and the growth rate of ice crystals is found to be fastest at −14 °C due to the possible effect of the quasi-liquid-layer under the given conditions.

Our study paves the way for understanding the fundamental issues in such a gas–solid phase transition with rational experimental design.

ASSOCIATED CONTENT

Supporting Information

The Supporting Information is available free of charge on the ACS Publications website.

ESEM micrographs under various conditions (PDF) Movie S1 showing step-by-step growth of ice-layer.

AUTHOR INFORMATION

Corresponding Authors

*E-mail: feilinfeng@gmail.com (L.F.).

*E-mail: wangyu@ncu.edu.cn (Y.W.).

Author Contributions

Y.W. conceived the idea for the project. Y.W. and Z.Z. designed the experiments. Z.Z. and D.L. conducted experiments. Z.Z., L.F., Z.R., and C.W.L. performed data analysis. Z.Z. and L.F. wrote the manuscript with help and input from all authors. All authors have given approval to the final version of the manuscript. Notes The authors declare no competing financial interest.

ACKNOWLEDGMENTS

This paper is dedicated in memory of Professor Yu Wang. We acknowledge the use of facilities in the Institute of High Sciences of Nanchang University, Jiangxi Provincial Key Laboratory of

Two-dimensional Materials and Devices, and Jiangxi Provincial Laboratory of Advanced Thin Film Technology. Financial support from the National Science Foundation of China (project nos. 51562026 and 11574126) and Jiangxi's Natural Science Foundation (project nos. 20171ACB20006 and 20171BAB216011) is also acknowledged.

Graphical abstract

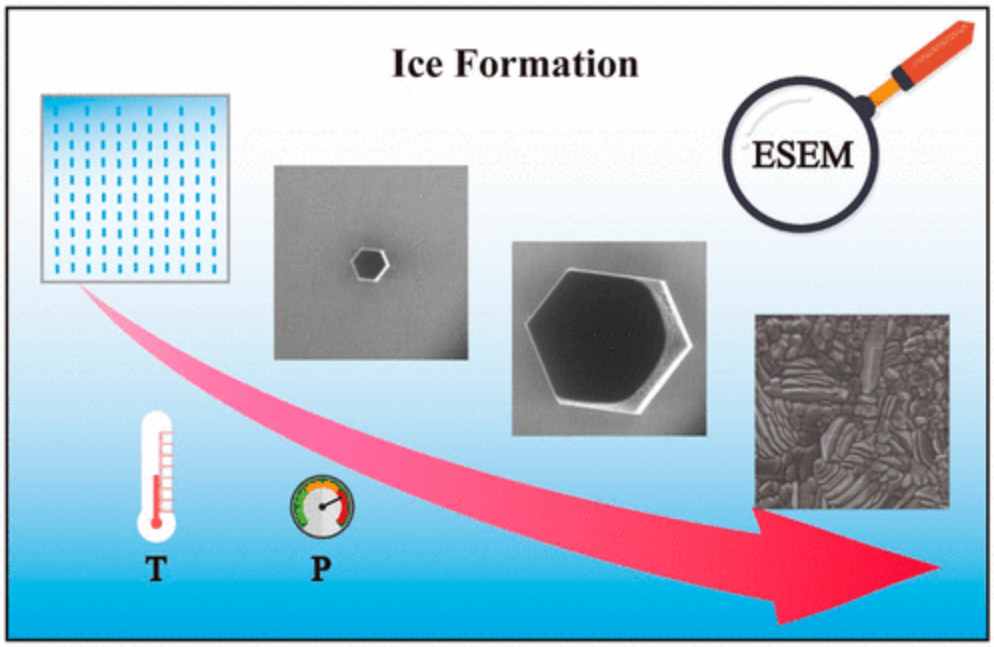

The microscopic growth process of ice through condensation of water vapor was, qualitatively and quantitatively, observed at different temperatures and saturations using an environmental scanning electron microscope (ESEM).

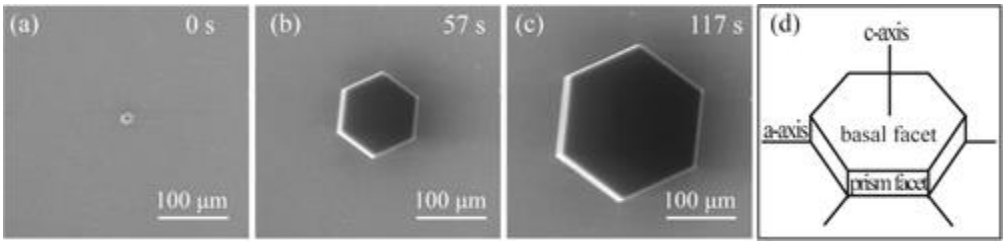

Figure 1. ESEM micrographs on growth dynamics of an ice crystal under $T = -15$ °C, $P = 179$ Pa, and $\sigma = 0.86\%$ at (a) 0 s, (b) 57 s, and (c) 117 s. (d) Schematic illustration of a basic hexagonal prism.

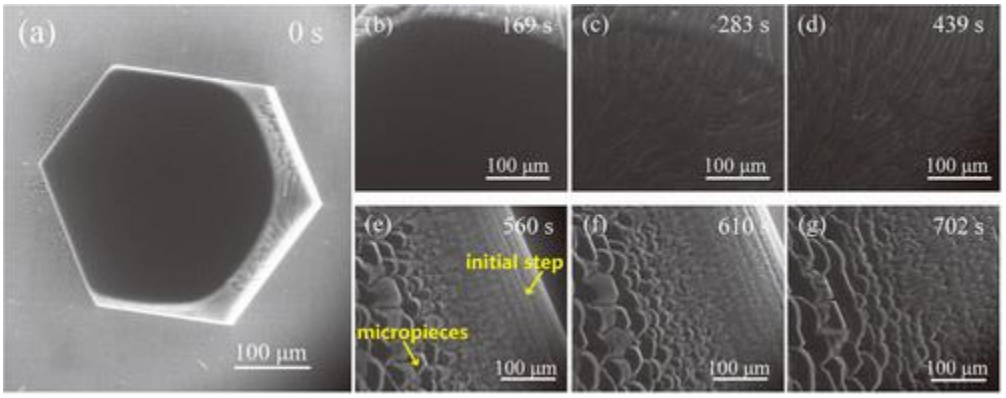

Figure 2. ESEM images show detailed morphological changes of two kinds of surfaces on an ice crystal under $T = -15$ °C, $P = 180$ Pa, and $\sigma = 1.20\%$. (a) Ice crystal with the outline as a hexagonal prism. (b–d) The changes of basal facet as a function of time. (e–g) Changes of the edge of prism facets as a function of time.

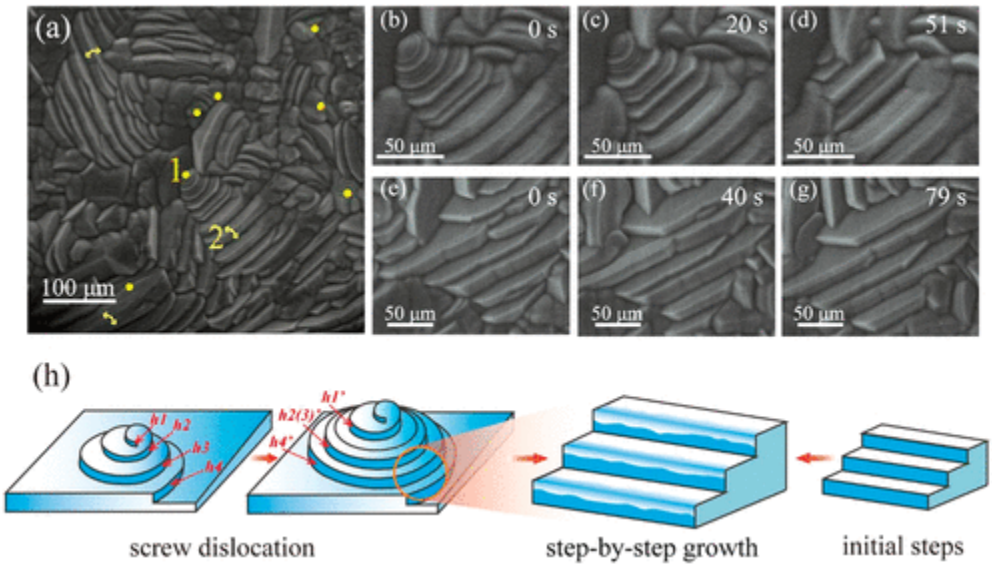

Figure 3. ESEM micrographs of the step-by-step growth of the ice-layer under $T = -13$ °C, $P =$ 230 Pa, and $\sigma = 15.68\%$. (a) Overview of a group of ice-layers. The yellow dots denote the head of the screw dislocations, and the yellow arrows denote single steps. Arabic numerals 1 and 2 denote screw dislocation and growth step of ice-layers, respectively. (b–d) Typical process of steps formation from a screw dislocation. (e–g) The growth pattern of steps during the ice-layer growth. (h) Schematic illustrations of the growth mechanism. h1, h2, h3, h4, and h1′, h2(3)′, h4′ denote the stages before and after the growth, respectively, in which h1 grew to h1′, h2 and h3 merged into one step of h2(3)′, and h4 evolved to h4′.

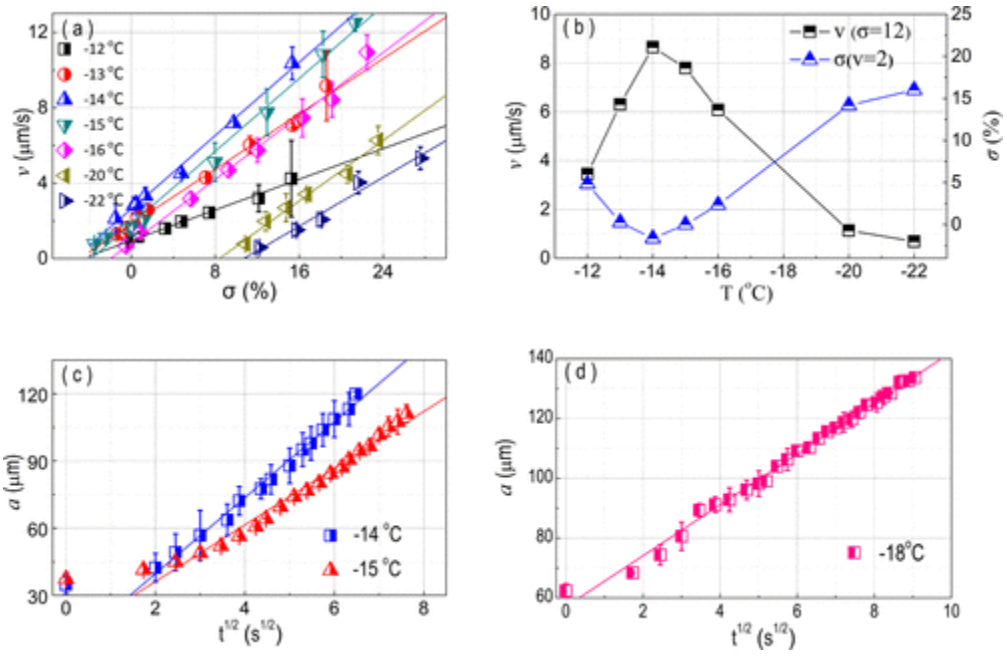

Figure 4. Statistical data during the growth of ice. (a) Dependence of the velocity (v) on supersaturation (σ) under different temperatures (T). (b) Dependence of σ (at a given v = 2 μm/s) and v (at a given σ = 12%) on T. (c) Relationship between the edge-length of basal facet and the time under the different temperatures at a given σ < 1% (σ at −14 °C and −15 °C are 0.27% and 0.20%, respectively). (d) The same relationship under −18 °C at a given σ = 8.65%.

Reference

(1) Cao, Y.; Wu, Z.; Su, Y.; Xu, Z. Aircraft Flight Characteristics in Icing Conditions. Progress in Aerospace Sciences 2015, 74, 62−80.

(2) Jung, S.; Tiwari, M. K.; Doan, N. V.; Poulikakos, D. Mechanism of Supercooled Droplet Freezing On Surfaces. Nat. Commun. 2012, 3, 615.

(3) Andersson, A. K.; Chapman, L. The Impact of Climate Change On Winter Road Maintenance and Traffic Accidents in West Midlands, UK. Accid. Anal. Prev. 2011, 43, 284−289.

(4) Golovin, K.; Kobaku, S. P. R.; Lee, D. H.; Diloreto, E. T.; Mabry, J. M.; Tuteja, A. Designing Durable Icephobic Surfaces. Sci. Adv. 2016, 2, e1501496.

(5) Mason, B. J. The Physics of Clouds; Clarendon Press: Oxford, 1971; Vol. 671, Issue 1, p 41.

(6) Libbrecht, K. G. The Physics of Snow Crystals. Rep. Prog. Phys. 2005, 68, 855−895.

(7) Libbrecht, K. G. A Critical Look at Ice Crystal Growth Data. Physics 2004.

(8) Colbeck, S. C. Ice Crystal Morphology and Growth Rates at Low Supersaturations and High Temperatures. J. Appl. Phys. 1983, 54, 2677−2682.

(9) Frank, F. C. Snow Crystals. Contemp. Phys. 1982, 23, 3−22.

(10) Humphreys, W. J. Snow Crystals; McGraw-Hill Book Company, 1931; pp 3−22.

(11) Nakaya, U. Frontmatter: Snow Crystals Natural and Artificial. Dictionary of Minor Planet Names 1954, 83, 119−120.

(12) Libbrecht, K. G. Morphogenesis On Ice: The Physics of Snow Crystals. Eng. Sci. 2001, 10−19.

(13) Magono, C. Meteorological Classification of Snow Crystals. J. Japanese Assoc. Snow Ice 1962, 24, 33−37.

(14) Gonda, T.; Yamazaki, T. Morphology of Ice Droxtals Grown From Supercooled Water Droplets. J. Cryst. Growth 1978, 45, 66−69.

(15) Aoki, K.; Katayama, K.; Hayashi, Y. A Study On Frost Formation: The Process of Frost Formation Involving the Phenomena of Water Permeation and Freezing. Bull. JSME 1983, 26, 87−93.

(16) Brian, P.; Reid, R. C.; Shah, Y. T. Frost Deposition On Cold Surfaces. Ind. Eng. Chem. Fundam. 1970, 9, 375−380.

(17) Sanders, C. T. The Influence of Frost Formation and Defrosting On the Performance of Air Coolers. Thesis, Technische Hogeschool, 1974.

(18) Yokoyama, E.; Kuroda, T. Pattern Formation in Growth of Snow Crystals Occurring in the Surface Kinetic Process and the Diffusion Process. Phys. Rev. A: At., Mol., Opt. Phys. 1990, 41, 2038.

(19) Shimada, W.; Furukawa, Y. Pattern Formation of Ice Crystals during Free Growth in Supercooled Water. J. Phys. Chem. B 1997, 101, 6171.

(20) Wood, S. E.; Baker, M. B.; Calhoun, D. New Model for the Vapor Growth of Hexagonal Ice Crystals in the Atmosphere. J. Geophys. Res. Atmos. 2001, 106, 4845−4870.

(21) Libbrecht, K. G. Physical Dynamics of Ice Crystal Growth. Annu. Rev. Mater. Res. 2017, 47, 271.

(22) Na, B.; Webb, R. L. A Fundamental Understanding of Factors Affecting Frost Nucleation. Int. J. Heat Mass Transfer 2003, 46, 3797− 3808.

(23) Na, B.; Webb, R. L. Mass Transfer On and within a Frost Layer. Int. J. Heat Mass Transfer 2004, 47, 899−911.

(24) Na, B.; Webb, R. L. New Model for Frost Growth Rate. Int. J. Heat Mass Transfer 2004, 47, 925−936.

(25) Lupi, L.; Hudait, A.; Peters, B.; Grünwald, M.; Gotchy Mullen, R.; Nguyen, A. H.; Molinero, V. Role of Stacking Disorder in Ice Nucleation. Nature 2017, 551, 218−222.

(26) Wu, X.; Dai, W.; Xu, W.; Tang, L. Mesoscale Investigation of Frost Formation On a Cold Surface. Exp. Therm. Fluid Sci. 2007, 31, 1043−1048.

(27) Wu, X.; Dai, W. T.; Shan, X. F.; Wang, W.; Tang, L. M. Visual and Theoretical Analyses of the Early Stage of Frost Formation on Cold Surfaces. J. Enhanced Heat Transfer 2007, 14, 257−268.

(28) Liu, J.; Zhu, C.; Liu, K.; Jiang, Y.; Song, Y.; et al. Distinct Ice Patterns On Solid Surfaces with Various Wettabilities. Proc. Natl. Acad. Sci. U. S. A. 2017, 114, 11285.

(29) Reiter, C. A. A Local Cellular Model for Snow Crystal Growth. Chaos, Solitons Fractals 2005, 23, 1111−1119.

(30) Hagiwara, Y.; Ishikawa, S.; Kimura, R.; Toyohara, K. Ice Growth and Interface Oscillation of Water Droplets Impinged On a Cooling Surface. J. Cryst. Growth 2017, 468, 46−53.

(31) Liu, K.; Wang, C.; Ma, J.; Shi, G.; Yao, X.; Fang, H.; Song, Y.; Wang, J. Janus Effect of Antifreeze Proteins On Ice Nucleation. Proc. Natl. Acad. Sci. U. S. A. 2016, 113, 14739.

(32) Yang, H.; Ma, C.; Li, K.; Liu, K.; Loznik, M.; Teeuwen, R.; Van Hest, J. C. M.; Zhou, X.; Herrmann, A.; Wang, J. Tuning Ice Nucleation with Supercharged Polypeptides. Adv. Mater. 2016, 28, 5008.

(33) Fei, L. F.; Sun, T. Y.; Lu, W.; An, X. Q.; Hu, Z. F.; Yu, J. C.; Zheng, R. K.; Li, X. M.; Chan, H. L.; Wang, Y. Direct Observation of Carbon Nanostructure Growth at Liquid-Solid Interfaces. Chem. Commun. 2014, 50, 826−828.

(34) Fei, L.; Ng, S. M.; Lu, W.; Xu, M.; Shu, L.; Zhang, W.; Yong, Z.; Sun, T.; Lam, C. H.; Leung, C. W.; Mak, C. L.; Wang, Y. AtomicScale Mechanism on Nucleation and Growth of Mo2C Nanoparticles Revealed by in Situ Transmission Electron Microscopy. Nano Lett. 2016, 16, 7875−7881.

(35) Fei, L.; Lei, S.; Zhang, W.; Lu, W.; Lin, Z.; Lam, C. H.; Chai, Y.; Wang, Y. Direct TEM Observations of Growth Mechanisms of Two-Dimensional MoS2 Flakes. Nat. Commun. 2016, 7, 12206.

(36) Fei, L.; Lu, W.; Hu, Y.; Gao, G.; Yong, Z.; Sun, T.; Zhou, N.; Gu, H.; Wang, Y. Evidencing the Structural Conversion of Hydrothermally Synthesized Titanate Nanorods by in Situ Electron Microscopy. J. Mater. Chem. A 2017, 5, 3786−3791.

(37) Danilatos, G. D. Introduction to the ESEM Instrument. Microsc. Res. Tech. 1993, 25, 354−361.

(38) Muscariello, L.; Rosso, F.; Marino, G.; Giordano, A.; Barbarisi, M.; Cafiero, G.; Barbarisi, A. A Critical Overview of ESEM Applications in the Biological Field. J. Cell. Physiol. 2005, 205, 328−334.

(39) Danilatos, G. D. Review and Outline of Environmental SEM at Present. J. Microsc. 1991, 162, 391−402.

(40) Stokes, D. J. Recent Advances in Electron Imaging, Image Interpretation and Applications: Environmental Scanning Electron Microscopy. Philos. Trans. R. Soc., A 2003, 361, 2771−2787.

(41) Donald, A. M. The Use of Environmental Scanning Electron Microscopy for Imaging Wet and Insulating Materials. Nat. Mater. 2003, 2, 511−516.

(42) Bergmans, L.; Moisiadis, P.; Van Meerbeek, B.; Quirynen, M.; Lambrechts, P. Microscopic Observation of Bacteria: Review Highlighting the Use of Environmental SEM. Int. Endod. J. 2005, 38, 775−788.

(43) Kiselev, A.; Bachmann, F.; Pedevilla, P.; Cox, S. J.; Michaelides, A.; Gerthsen, D.; Leisner, T. Active Sites in Heterogeneous Ice Nucleation-The Example of K-rich Feldspars. Science 2017, 355, 367.

(44) Cheng, Y.; Rodak, D. E.; Angelopoulos, A.; Gacek, T. Microscopic Observations of Condensation of Water On Lotus Leaves. Appl. Phys. Lett. 2005, 87, 194112.

(45) Miljkovic, N.; Enright, R.; Wang, E. N. Effect of Droplet Morphology On Growth Dynamics and Heat Transfer During Condensation On Superhydrophobic Nanostructured Surfaces. ACS Nano 2012, 6, 1776−1785.

(46) Wang, B.; Knopf, D. A.; China, S.; Arey, B. W.; Harder, T. H.; Gilles, M. K.; Laskin, A. Direct Observation of Ice Nucleation Events On Individual Atmospheric Particles. Phys. Chem. Chem. Phys. 2016, 18, 29721.

(47) Ketcham, W. M.; Hobbs, P. V. Step Growth On Ice During the Freezing of Pure Water. Philos. Mag. 1968, 18, 659−661.

(48) Lamb, D.; Scott, W. D. The Mechanism of Ice Crystal Growth and Habit Formation. J. Atmos. Sci. 1974, 31, 570−580.

(49) Nada, H.; Furukawa, Y. Anisotropic Growth Kinetics of Ice Crystals From Water Studied by Molecular Dynamics Simulation. J. Cryst. Growth 1996, 169, 587−597.

(50) Libbrecht, K. Growth Rates of the Principal Facets of Ice Between −10 °C and −40°C. J. Cryst. Growth 2003, 247, 530−540.

(51) Dosch, H.; Lied, A.; Bilgram, J. H. Glancing-Angle X-ray Scattering Studies of the Premelting of Ice Surfaces. Surf. Sci. 1995, 327, 145−164.

(52) Petrenko, V. F. Physics of Ice; Oxford, 1999.

(53) Dash, J. G.; Rempel, A. W.; Wettlaufer, J. S. The Physics of Premelted Ice and its Geophysical Consequences. Rev. Mod. Phys. 2006, 78, 695−741.